brief communication

Metastable ripple phase of fully hydrated dipalmitoylphosphatidylcholine as studied by small angle x-ray scattering

Haruhiko Yao,* Sinzi Matuoka,* Boris Tenchov,‡ and Ichiro Hatta*

*Department of Applied Physics, Nagoya University, Nagoya 464-01, Japan; and ‡Central Laboratory of Biophysics, Bulgarian Academy of Sciences, 1113 Sofia, Bulgaria

ABSTRACT Fully hydrated dipalmitoylphosphatidylcholine (DPPC) undergoes liquid crystalline to metastable $P_{\beta'}$ phase transition in cooling. A small angle x-ray scattering study has been performed for obtaining further evidence about the structure of this phase. From a high-resolution observation of x-ray diffraction profiles, a distinct multipeak pattern has become obvious. Among them the (01) reflection in the secondary ripple structure is identified clearly. There are peaks assigned straightforwardly to (10) and (20) reflections in the primary ripple structure and peaks assigned to (10) and (20) reflections in the secondary ripple structure. Therefore the multipeak pattern is due to superposition of the reflections cause by the primary and secondary ripple structures. The lattice parameters are estimated as follows: for the primary ripple structure $a = 7.09$ nm, $b = 13.64$ nm, and $\gamma = 95°$, and for the secondary ripple structure $a = 8.2$ nm, $b = 26.6$ nm, and $\gamma = 90°$. The lattice parameters thus obtained for the secondary ripple structure are not conclusive, however. The hydrocarbon chains in the primary ripple structure have been reported as being tilted against the bilayer plane and, on the other hand, the hydrocarbon chains in the secondary ripple structure are likely to be perpendicular to the bilayer plane. This fact seems to be related to a sequential mechanism of phase transitions. On heating from the $L_{\beta'}$ phase where the hydrocarbon chains are tilted the primary ripple structure having tilted hydrocarbon chains takes place and on cooling from the L_α phase where the hydrocarbon chains are not tilted the secondary ripple structure with untilted chains tends to be stabilized. It appears that the truly metastable ripple phase is expressed by the second ripple structure although in the course of the actual cooling transition both the secondary and primary ripple structures form and coexist.

INTRODUCTION

In our recent paper (Tenchov et al., 1989), we have pointed out, on basis of x-ray diffraction, high-sensitive differential scanning calorimetry and ac calorimetry studies of fully hydrated dipalmitoylphosphatidylcholine (DPPC), that the main transition of DPPC is not reversible in the sense that the initial $P_{\beta'}$ phase, appearing on heating from the $L_{\beta'}$ phase, does not reappear on cooling from the L_α phase, but is replaced by a metastable phase $P_{\beta'}$(mst).

The metastable $P_{\beta'}$ phase is long living under keeping constant temperature but can be converted readily to the initial $P_{\beta'}$ phase by cooling to the $L_{\beta'}$ phase and subsequent reheating through the pretransition. It has been made clear by calorimetry that the enthalpy of the $P_{\beta'}$(mst) phase is 0.4 kcal/mol higher than that of the $P_{\beta'}$ phase, that is, the $P_{\beta'}$(mst) phase should be considered as metastable in comparison with the initial $P_{\beta'}$ phase. In the small angle x-ray scattering a complex profile appears in cooling which is different from that of the initial $P_{\beta'}$ phase and consists of multipeaks with low intensity. The difference in x-ray diffraction patterns suggests that the $P_{\beta'}$(mst) phase should be less ordered with respect to correlation and/or stacking of the bilayers. Once the less-ordered $P_{\beta'}$(mst) state is formed, conversion to the ordered $P_{\beta'}$ state is strongly hindered notwithstanding the small enthalpy difference. However, the multiple diffraction peaks were not elucidated in detail.

In the $P_{\beta'}$ phase of DPPC a ripple structure with the wavelength of ~13 nm has been observed by freeze-fracture electron microscopy (Luna and McConnell, 1977) and x-ray diffraction (Janiak et al., 1976). In addition to this primary ripple structure, a secondary ripple structure with approximately twofold wavelength has been found by freeze-fracture electron microscopy (Hicks et al., 1987), although the conditions for its appearance have not been clarified. Very recently, in connection with the existence of $P_{\beta'}$(mst) observations by freeze-fracture electron microscopy were carried out in our laboratory. It was found that the primary ripple structure took place mostly when the replica was made by quenching the DPPC vesicles from the $P_{\beta'}$ phase during the course of a slow heating run from the $L_{\beta'}$ phase and on the other hand, the secondary ripple structure was widely present when in the same temperature range the replica was made by quenching the DPPC vesicles during the course of a slow cooling run from the L_α phase. The details of this result will be published

Address correspondence to Ichiro Hatta, Department of Applied Physics, Nagoya University, Nagoya 464-01, Japan.

0006-3495/91/01/252/04 $2.00

elsewhere (Kato, S., K. Miyazawa, H. Miyamoto, K. Honda, and I. Hatta, manuscript in preparation).

In this paper, the small-angle synchrotron x-ray scattering study was reexamined by paying attention to the very small angle region, where diffraction caused by longer ripple regular distance could be expected, and the assignment of the multipeaks was considered.

MATERIALS AND METHODS

DPPC (1,2-dipalmitoyl-*sn*-glycero-3-phosphocholine) was obtained from Avanti Polar Lipids Inc. (Burmingham, AL). The method of sample preparation was the same as described previously (Tenchov et al., 1989). Multilamellar lipid vesicles were prepared in 65 wt% bidistilled deionized water. This certainly satisfies the condition for excess water (Kodama et al., 1982). Synchrotron x-ray diffraction experiments were carried out using a monochromatic x-ray beam with wavelength $\lambda = 0.155$ nm at Station 15A of the Photon Factory (PF). The optical system and sample setting were also similar to those previously used (Tenchov et al., 1989). Diffraction patterns were recorded using a one-dimensional position sensitive proportional counter (Rigaku, Tokyo). In the present study, the diffraction patterns were taken at ~40°C during the course of a heating run from the $L_{\beta'}$ phase and a cooling run from the L_{α} phase at a scan rate of 0.1 °C/min.

RESULTS AND DISCUSSION

The x-ray diffraction profiles of DPPC/water at 40°C obtained during slow heating and slow cooling scans are quite different as seen in Figs. 1 and 2, respectively. As noted in our previous paper (Tenchov et al., 1989), a slow scan experiment seems to be important to get a highly resolved diffraction profile. It has been clarified that in a slow heating scan a standard diffraction profile appears in the $P_{\beta'}$ phase and, on the other hand, in a slow cooling scan a complicated multipeak diffraction profile takes place at the same temperature. We called the latter a metastable $P_{\beta'}$ phase. However, the origin of this profile remained unclear.

TABLE 1 Indexing in the two-dimensional unit cell (hk) for the diffraction of the ripple phase in heating

Peak no.	d_{obs}	d_{cal} (hk)
	nm	*nm*
1	13.90 ± 0.4	14.0 (01)
2	7.16 ± 0.1	7.06 (10)
3	6.27 ± 0.07	6.18 (11)
4	3.53 ± 0.02	3.53 (20)
5	3.36 ± 0.02	3.38 (21)

Peak nos. 1–5 correspond to nos. 1–5 in Fig. 1, respectively. The estimated lattice parameters are: $a = 7.06$ nm, $b = 14.00$ nm, and $\gamma = 92.9°$ and the calculated spacings d_{cal} are given together with the observed ones d_{obs}.

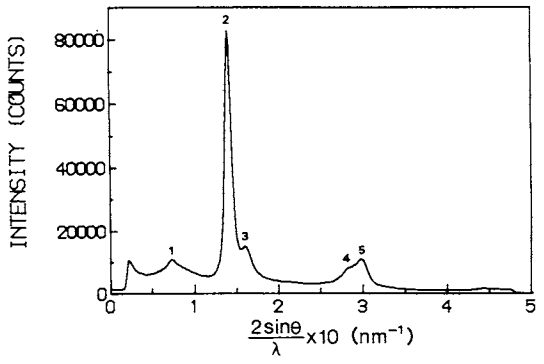

FIGURE 1 Diffraction profile in the ripple phase at 40°C taken during the course of a heating run. For the peaks denoted by nos. 1–5, see text and Table 1.

To study this behavior in detail, the 25 profiles at ~40°C were added up in the results obtained for heating (Fig. 1) and cooling (Fig. 2). The standard deviation of the intensity in each profile was ~35 counts and then the data accumulation reduces the scatter of the intensity markedly. Peak No. 1 in Fig. 2 is especially not obvious until the accumulation. We first discuss the pattern in Fig. 1. The assignment of the peaks denoted by 1–5 in Fig. 1 is given in Table 1. In a two-dimensional lattice, the estimated lattice parameters are $a = 7.06$ nm and $b = 14.00$ nm and the angle is 92.9°. This almost agrees with the result obtained for 66.8% wt% DPPC/33.2 wt% water by Wack and Webb (1989). For further consideration, care should be taken for water concentration. From the differential scanning calorimetry study (Kodama et al., 1982), it has been deduced that the condition for excess water is satisfied at water concentration above 50 wt%. So far x-ray diffraction studies on the DPPC/water system have been carried out by many researchers. The results of Janiak et al. (1976) indicate that the lattice parameters become constant at the water concentrations more than 25 wt%. On the other hand, the results of Wack and Webb (1989) show gradual change up to 33.2% water. The lattice parameters obtained by Wack and Webb (1989) are 6.878 and 14.19 nm and the angle is 92.85° in the sample with 33.2 wt% water. According to their result, the smaller lattice constant increases, the larger decreases, and the angle decreases but scatters with increase of water concentration. This tendency might be extended to water concentrations over 33.2 wt%. Consequently our present result for excess water of 65 wt% is consistent with the result expected from the data of Wack and Webb (1989).

The profile in Fig. 2 in cooling appears to be complicated. Comparing Figs. 1 and 2, we find some coincidence in the peak positions: No. 1 of Fig. 1 corresponds

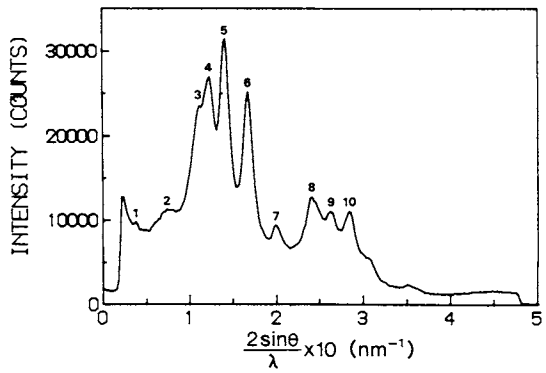

FIGURE 2 Diffraction profile in the ripple phase at 40° taken during the course of a cooling run. For the peaks denoted by nos. 1–10, see text and Table 2.

to No. 2 of Fig. 2; No. 2 to No. 5; No. 3 to No. 5; No. 4 to No. 10. The remaining peaks in Fig. 2 are Nos. 1, 3, 4, 7, 8, and 9. It is important to note that No. 1 of lattice spacing 26.4 ± 0.7 nm in Fig. 2 coincides with the ripple repeat distance for the secondary ripple structure. This is the first observation of the secondary ripple peak by x-ray diffraction. The appearance of this peak is consistent with the result of our recent electron micrograph (Kato, S., K. Miyazawa, H. Miyamoto, K. Honda, and I. Hatta, manuscript in preparation). It is conceivable that the broad peak No. 2 at 14.3 ± 0.4 nm in Fig. 2 should be assigned not only to the (01) reflection the primary ripple structure but also to the (02) reflection for the secondary ripple structure. The reason why the profile exhibits a broad maximum seems to be partly due to the superposition of the above two different reflections. The spread of the peak is caused also by a less-ordered bilayer stacking. Peak No. 3 at 9.0 ± 0.2 nm in Fig. 2 seems to correspond to the (03) reflection of the secondary structure. In Fig. 2 the assignment of the (10) reflections for the primary and secondary ripple structure is rather straightforward because in these cases the lattice spacings for the (20) reflections should be found at twice as large as those for the (10) reflections. Actually, the lattice spacings for (10) and (20) for the primary ripple structure are 7.16 ± 0.10 and 3.52 ± 0.02 nm and those for the secondary ripple structure are 8.22 ± 0.17 and 4.14 ± 0.03 nm, respectively. Thus, No. 5 of Fig. 2 can be assigned to (10) for the primary ripple structure and No. 10 to (20). Furthermore, No. 4 of Fig. 2 can be assigned to (10) for the secondary ripple structure and No. 8 to (20). The obtained spacings of (10) and (20) for the primary ripple structure in Fig. 2 agree with those in Fig. 1.

To explain the above reflections and the remaining reflections consistently the lattice constants obtained in cooling are estimated to be a = 7.09 nm and b = 13.64 nm with $\gamma = 95°$ for the primary ripple structure and a = 8.2 nm and b = 26.6 nm with $\lambda = 90°$ for the secondary ripple structure. The list of observed and calculated lattice spacings and possible assignment is given in Table 2. However, some of the assignments are still uncertain. They are distinguished with asterisk in Table 2. The position of peak No. 3 in Fig. 2 assigned to (03) of the secondary ripple structure is uncertain as it is located on the slope of peak No. 4. Furthermore it should be noted that around No. 3 and/or slightly below this angle a broad hump was observed in some of the experiments. This seems to indicate that the stacking of the multibilayers is markedly irregular and the irregularity changes from one experiment to another. This is consistent with a coexistence of the primary and the secondary ripple structures resulting in a large number of discontinuities at their boundaries. It is concluded that a broad reflection of this type is caused by disorder in stacking and that it lies at a lower angle in comparison with the normal (10) reflection due to bigger and scattered spacing. The intensity of peak No. 6 in Fig. 2 assigned to (11) of the primary ripple structure is also big when compared with (11) reflection in Fig. 1. Thus it is not clear whether the above assignment is convincing enough or not at present.

Within the framework of a sequential mechanism which has been proposed in our previous paper (Tenchov et al., 1989) we consider now the hysteresis in the appearance of the ripple structures. This mechanism

TABLE 2 Indexing in the two-dimensional unit cell (hk) for the diffraction of the ripple phase in cooling

Peak no.	d_{obs}	Primary ripple structure d_{cal} (hk)	Secondary ripple structure d_{cal} (hk)
	nm	*nm*	*nm*
1	26.38 ± 0.7		26.6 (01)
2	14.32 ± 0.4	14.0 (01)	
3	8.95 ± 0.2		8.87 (03)*
4	8.22 ± 0.17		8.30 (10)
5	7.16 ± 0.10	7.06 (10)	
6	5.97 ± 0.07	6.05 (11)*	
7	5.06 ± 0.05	5.12 (1–2)*	
8	4.14 ± 0.03		4.15 (20)
9	3.83 ± 0.03		3.83 (22)*
10	3.53 ± 0.02	3.53 (20)	

Peak nos. 1–10 correspond to nos. 1–10 in Fig. 2, respectively. The profile is a superposition of two sets of reflections originating from the primary and secondary ripple structure. The estimated lattice parameters for the primary ripple structure are: a = 7.09 nm, b = 13.64 nm, and $\gamma = 95°$ and for the secondary ripple structure: a = 8.2 nm, b = 26.6 nm, and $\gamma = 90°$. The observed spacing d_{obs} and the calculated spacings d_{cal} are given. The assignment of reflection (hk) denoted by * is not conclusive.

gives rise to dependence of a given state on the structure of a phase preceding in time. This might be the case in the appearance of the present ripple structures: in heating, the ripple formation starts from the $L_{\beta'}$ phase where the hydrocarbon chains are tilted and the primary ripple structure in which the hydrocarbon chains are tilted as well follows as a necessary consequence; on the other hand, in cooling, the ripple formation starts from the L_{α} phase in which the hydrocarbon chains are perpendicular to the bilayer plane and then the symmetric secondary ripple structure with hydrocarbon chains perpendicular to the bilayer plane might be formed with reflecting the lack of tilt in the preceding phase. In cooling, the secondary ripple structure seems to form together with the stable primary ripple structure. Therefore, it is very likely that the truly metastable phase is formed only by the secondary ripple structure.

The authors thank Professor M. Akiyama and Dr. S. Kato for valuable discussions and Dr. Y. Amemiya for advice in the instrumentation of synchrotron x-ray scattering experiments.

One of the authors (Dr. Yao) is indebted to the support by a grant-in-aid for Encouragement of Young Scientists from the Ministry of Education, Science, and Culture of Japan.

Received for publication 4 June 1990 and in final form 30 August 1990.

REFERENCES

Hicks, A., M. Dinda, and M. A. Singer. 1987. The ripple phase phosphatidylcholines: effect of chain length and cholesterol. *Biochim. Biophys. Acta.* 903:177–185.

Janiak, M. J., D. M. Small, and G. G. Shipley. 1976. Nature of the thermal pretransition of synthetic phospholipids: dimyristoyl- and dipalmitoyllecithin. *Biochemistry.* 15:4575–4580.

Kodama, M., M. Kuwabara, and S. Seki. 1982. Successive phase transition phenomena and phase diagram of the phosphatidylcholine-water system as revealed by differential scanning calorimetry. *Biochim. Biophys. Acta.* 689:567–570.

Luna, E. J., and H. M. McConnell. 1977. The intermediate monoclinic phase of phosphocholines. *Biochim. Biophys. Acta.* 466:381–392.

Tenchov, B. G., H. Yao, and I. Hatta. 1989. Time-resolved x-ray diffraction and calorimetric studies at low scan rates I. Fully hydrated dipalmitoylphosphatidylcholine (DPPC) and DPPC/water/ethanol phases. *Biophys. J.* 56:757–768.

Wack, D. C., and W. W. Webb. 1989. Synchrotron x-ray study of the modulated lamellar phase $P_{\beta'}$ in the lecithin-water system. *Phys. Rev. A.* 40:2712–2730.